Regular Article

PHYSICAL CHEMISTRY RESEARCH
Published by the
Iranian Chemical Society
www.physchemres.org
info@physchemres.org

Phys. Chem. Res., Vol. 13, No. 4, 623-630, December 2025
DOI: 10.22036/pcr.2025.515150.2670

Uneven Distributions of Electrons and Holes in Polycyclic Systems Exposed to Electric Field

F. Hajipour and S.M. Azami*
Department of Chemistry, College of Sciences, Yasouj University, Yasouj, Iran
(Received 5 April 2025, Accepted 23 June 2025)

Dedicated to the late Professor A. H. Pakiari of Shiraz University, an inspiring researcher and scientist, in recognition of his remarkable contributions to physical chemistry.

Polycyclic rhombus type conjugated systems from a small 4 hexagonal rings to 25 ring graphene flake are considered as candidate devices for electron transport, where electric field is applied along both diagonals to simulate potential difference. The electronic response to external electric field is analyzed *via* two types of deformation densities: the conventional electronic deformation originated from the electric field, and asymmetric deformation that reflects the way electrons and holes are distributed over the entire molecule. Conventional deformation density analysis shows even distribution of electrons and holes as mirror images. On the other hand, asymmetric analysis shows a wave-like texture for distribution of electrons and holes all over the molecule, however electrons tend to occupy apices and edges, while holes are localized in the central area.

Keywords: Polycyclic systems, Electrons and holes, Electric field, Deformation density, Asymmetric distribution

INTRODUCTION

Polycyclic systems, characterized by their multiple fused aromatic rings, exhibit delocalized π-electron clouds that facilitate charge transport [1,2]. When an electric field is applied, these delocalized electrons and their corresponding holes (the absence of an electron) redistribute, giving rise to interesting phenomena [3,4]. This redistribution is governed by a complex interplay of factors, including the molecular structure, the strength and direction of the electric field, temperature, and the presence of impurities or defects [5-7]. Understanding the behavior of charge carriers, namely electrons and holes, within these systems under the influence of an electric field is important for optimizing such devices' performance.

The movement of electrons and holes under an electric field, is quantified by their mobility, which reflects how easily they can move through the material [8-10]. Higher mobility translates to better charge transport and improved device performance, and is influenced by electronic structure properties of the molecular-scale devices. While application of an electric field induces polarization in the polycyclic system leading to the alignment of molecular dipoles, the dielectric constant as a measure of a material's ability to store electrical energy is related to the polarization; and affects the electrons and holes distribution within the material [11-13]. When the electric field is applied, electrons and holes experience a force that drives them towards opposite ends of the molecule, that results in a non-uniform charge distribution, creating regions of higher electron density and regions of higher hole density.

While symmetric molecules often exhibit uniform charge distribution, asymmetry imposes by the applied electric field can lead to an uneven distribution of electrons and holes [14,15]. The field induced response, breaks the symmetry of the molecular orbitals, leading to an uneven distribution of electron density. Consequently, the system's response to the external stimuli, such as light or electric fields, becomes anisotropic, exhibiting direction-dependent behavior. This asymmetry has profound implications for various

*Corresponding author. E-mail: azami@yu.ac.ir

applications, including organic electronics, photovoltaics, and nonlinear optics. Replacing carbon atoms with heteroatoms like nitrogen, oxygen, or sulfur also introduces differences in electron density distribution within the molecule [16-18]. Attaching electron-donating or electron-withdrawing groups to the polycyclic core can also significantly perturb the electron density distribution [19-22]. Electron-donating groups increase electron density in the conjugated system, while electron-withdrawing groups decrease it. Deviations from planarity, such as bending or twisting of the polycyclic structure, can also lead to asymmetric charge distribution [23,24]. These distortions can arise from steric hindrance between substituents or from interactions with the surrounding environment.

Asymmetric charge distribution results also in a permanent dipole moment, making the molecule polar. This polarity influences inter- and intra-molecular interactions, and can affect the molecular electronic structure and properties, *e.g.*, as a device in molecular electronics technology. The asymmetric distribution of charge carriers can also affect their mobility and transport properties [25-27]. For example, localized charge densities can act as traps, hindering charge transport, while directional charge transfer can be enhanced in specific directions [28,29].

While there exist too many publications on production of field-induced electron and hole, there exist few researches on symmetry of their distribution. In this respect, the present work aims at inspection of how electric field nests distinct area for electrons and holes in polycyclic conjugated systems.

COMPUTATIONAL DETAILS

Electronic wavefunctions are calculated at B3LYP/6-31G* level of theory [30,31], where C-C bond lengths are kept frozen to avoid geometrical deformation due to the applied electric field [14,15]. Electron density difference may not be a useful quantity, unless position of the nuclei share the same Cartesian coordinates in both states, which correspond to field-free and field-applied states in the present work. Therefore, molecular geometries are constrained to those geometries where no electric field exists. In order to simulate 1 V potential difference, electric field vector is applied along diagonals obeying E = V/d, where E and d denote magnitude of electric field and distance, respectively. The concept of electron deformation orbitals (EDOs) and eigenchannels [32-36] are used for response analysis of polycyclic systems to electric field, and asymmetric deformation density analysis [14,15] is used for determination of hole/electron asymmetry. Gaussian16 [37] is used for wavefunction calculations, Densitizer [38] is employed as a post-processing software for EDO and asymmetric deformation density analyses, and isosurfaces are plotted with the help of GaussView program [39].

RESULTS AND DISCUSSION

In this section, asymmetric deformation density analysis is performed on four aromatic polycyclic systems, containing 4, 9, 16, and, 25 aromatic hexagons and saturated by terminal hydrogens. These structures are shown in Fig. 1 as **S2** to **S4**, where xy-coordinates is orientated in a way that x and y axes coincide with long and short diagonals, respectively. While **S2** is a small aromatic molecule, **S5** resembles a graphene flake, and reasonable nanodevice for electron transport and molecular-scale transistors.

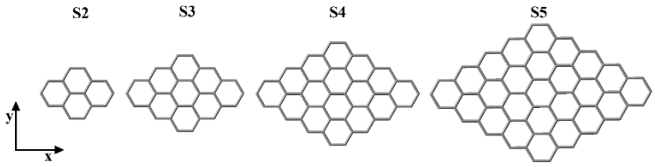

Fig. 1. Structures of the polycyclic systems along with considered xy-coordinates. Terminal hydrogen atoms are not shown for clarity.

To expose structures to 1 V potential difference, electric field vector is applied along both diagonals, where longest carbon-carbon distance in that diagonal alignment is taken into account for calculation of magnitude of electric field. In order to analyze how electrons and holes appear in distinct area of the structures, both conventional and asymmetric deformation density analyses are performed. Table 1 contains electronic deformation density isosurfaces originated from the electric field and the corresponding displaced charges (Δn) [14,15,32]. The Δn values lie in the range of 0.2 to 0.5 and are stronger in y-direction electric fields. Although distribution of electrons and holes in Table 1 as blue and yellow area seem to be symmetric with naked eyes, deeper look shows asymmetric distribution of these two, that can be revealed *via* asymmetric deformation density analysis [14,15].

Table 1. Electric Field Deformation Density Isosurfaces for **S2** to **S5** under 1 V Potential Difference, and their Displaced Charge (Δn) below the Surfaces. Blue and Yellow Colors Denote Charge Concentration and Depletion, Respectively

	S2	**S3**	**S4**	**S5**
Field(x)	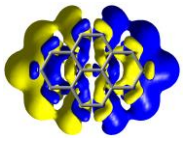 0.23	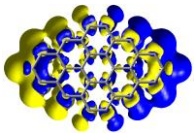 0.26	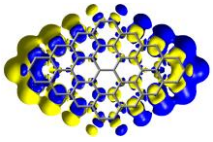 0.30	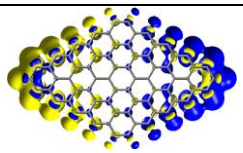 0.33
Field(y)	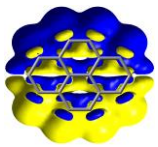 0.30	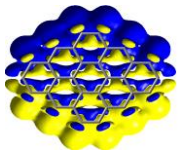 0.37	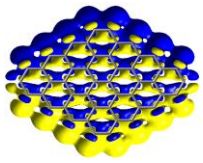 0.44	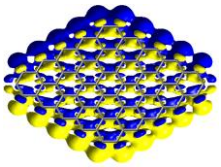 0.51

Table 2. Conventional and Asymmetric Deformation Density Isosurfaces for **S2** to **S5** ($x10^{-2}$) under 1 V Potential Difference, and their Displaced Charge (Δn) below the Surfaces. Blue and Yellow Colors Denote Charge Concentration and Depletion, Respectively

System	Single-direction		Asymmetric	
	Field (x)	Field (y)	Field (x)	Field (y)
S2	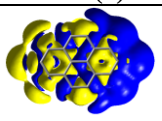 0.49	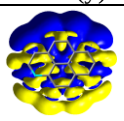 0.59	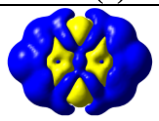 0.93	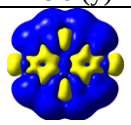 1.11
S3	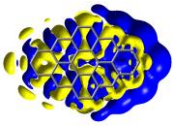 0.62	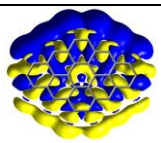 0.61	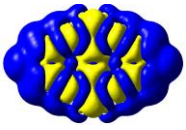 1.18	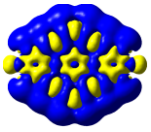 1.17
S4	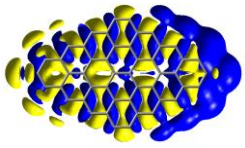 0.85	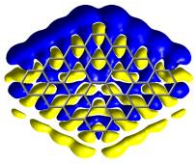 0.66	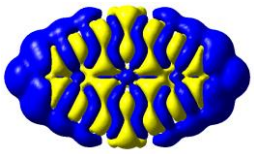 1.62	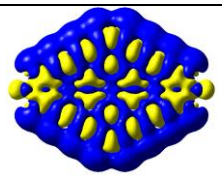 1.25
S5	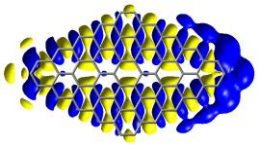 0.96	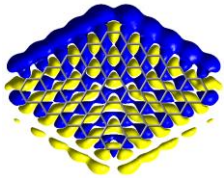 0.74	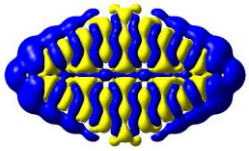 1.85	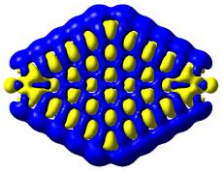 1.42

Table 2 displays two types of deformation densities isosurfaces for **S2** to **S5**, and their displaced charges values (Δn), where the structures experience 1 V potential difference along both of their diagonals: single-direction and asymmetric deformation densities. From now on, **x** and **y** suffixes are added to denote orientations of which the electric

field is applied along long and short diagonals, respectively, and Δn values are multiplied by 10^2. For example, **S2x** and **S2y** mean **S2** exposed to 1 V potential difference along x (long diagonal) and y (short diagonal) Cartesian axes, respectively, and Δn = 1 means 0.01 e charge displacement.

With respect to single-direction deformation density analysis entries in Table 2, Δn values grow with the molecular size, while not x-direction field values are greater than those of y-direction field (**S2** is an exception in which $\Delta n_x < \Delta n_y$). Both electron concentration and depletion (holes), denoted by blue and yellow colors, are appeared as a wave like texture in the isosurfaces of Table 2. Direction of the applied electric field is also clear from appearance of electrons and holes, as the electric field pushes charge from one apex to the opposite one. While electron concentration is highly concentrated around one apex, depending on the field direction, holes are distributed more evenly in all isosurfaces in this table. It is clear that electrons and holes do not comply to mirror images and tendency of electrons to occupy apices are obviously more than holes.

Table 2 also display asymmetric deformation density analysis including isosurfaces and their corresponding displaced charges. These analysis present asymmetric distribution of electrons and holes in another language, where blue and yellow colors directly point to how different apices are occupied by electrons and holes. It is evident from asymmetric deformation density isosurfaces that, charge tend to occupy apices and edges, while holes are concentrated at the center as a wave like structure. Also it can be seen that, electrons occupy a tiny area at the center of molecules, regardless of size and number of polygons.

Figure 2 shows occupancies of EDOs in field-free state in vertical axes, *i.e*., the system is exposed to no electric field, where EDOs are sorted with respect to their eigenvalues from 1 to 50 in the horizontal axes. In this figure, blue and orange colors stand for EDOs responsible for charge concentration and depletion, respectively. Asymmetric distribution of EDOs is also clear from the two blue and orange curves as they are not completely mirror images with respect to hypothetical horizontal line between the two colors. Such asymmetric distribution is more clear in the first EDOs of **S4y** and **S4x**, where possess highest eigenvalues than last EDOs at the end of curves.

SUMMARY AND CONCLUDING REMARKS

The asymmetric distribution of electrons and holes in polycyclic systems is a fascinating phenomenon with far-reaching consequences for the materials electronic and optical properties. This asymmetry can be introduced and controlled through various means, offering opportunities to tailor the materials' properties for specific applications. Advances in theoretical modeling, synthetic chemistry, and experimental characterization techniques are continuously expanding our understanding of these complex systems, paving the way for the development of novel materials and devices with enhanced performance and functionalities.

The distribution of electrons and holes in polycyclic systems under the influence of electric fields is a complex phenomenon governed by multitude of factors. It has been shown that, electrons and holes tend to occupy distinct locations of polycyclic systems and obey similar pattern for different molecular sizes, when exposed to an external electric field in the two directions. Electrons apt to locate at apices and edges, while holes try to be located at center and near to edge area. Occupancies of EDOs also show how electrons and holes are distributed asymmetrically among decomposition spectrum.

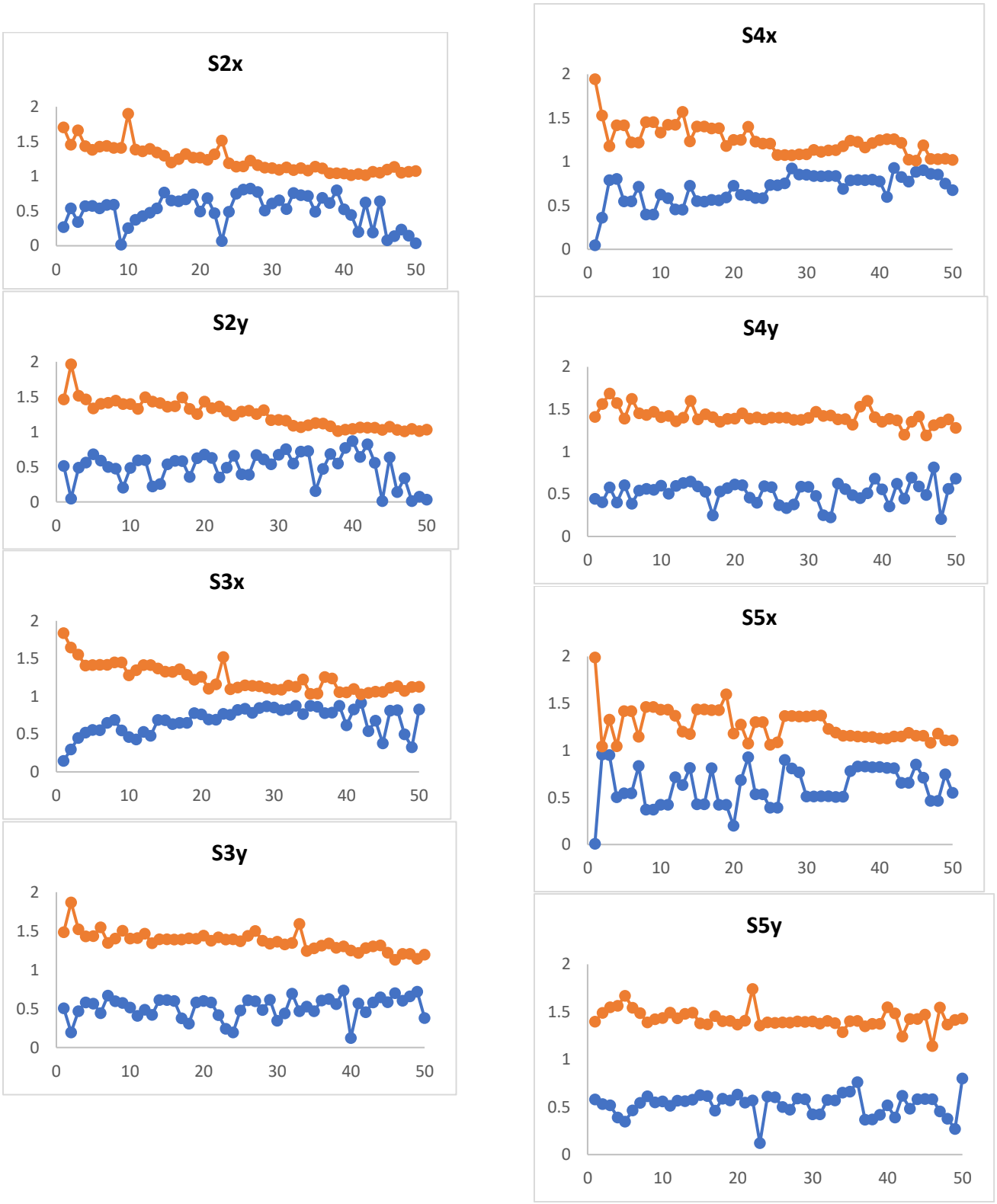

Fig. 2. Occupancy distribution of EDOs, where horizontal and vertical axes stand for sorted EDO numbers and occupancy, respectively. Blue and orange colors stand for EDOs responsible for charge concentration and depletion, respectively.

REFERENCES

[1] Quintero, S. M.; Nyvel L. V.; Roig, N.; Casado, J.; Alonso, M., Electron Transport through Linear-, Broken-, and Cross-Conjugated Polycyclic Compounds. *J. Phys. Chem. A* **2024**, *128*, 6140-57, DOI: 10.1021/acs.jpca.4c01588.

[2] Panahi, S. F. K. S.; Namiranian, A.; Soleimani, M.; Jamaati, M., Electron transport in polycyclic aromatic hydrocarbons/boron nitride hybrid structures: density functional theory combined with the nonequilibrium Green's function. *Phys. Chem. Chem. Phys*. **2018**, *20*, 4160-6, DOI: 10.1039/C7CP07260K.

[3] Plentz, F.; Heiman, D.; Pinczuk, A.; Pfeiffer, L. N.; West K. W., Electron-hole separation in a two-dimensional electron system induced by electric fields. *Solid State Commun*. **1997**, *101*, 103-7, DOI: 10.1016/S0038-1098(96)00559-5.

[4] Yamaguchi, M.; Nomura, S.; Miyakoshi, K.; Akazaki, T.; Tamura, H.; Takayanagi, H., Electric-field control of electron-hole wave functions in a wide quantum well. *Physica E* **2006**, *34*, 300-3, DOI: 10.1016/j.physe.2006.03.161.

[5] Sarkar, S.; Un, I. W.; Sivan, Y.; Dubi, Y., Theory of non-equilibrium 'hot' carriers in direct band-gap semiconductors under continuous illumination. *New J. Phys*. **2022**, *24*, 053008, DOI: 10.1088/1367-2630/ac6688.

[6] Ye, F.; Zhang, L.; Lu, C.; Bao, Z.; Wu, Z.; Liu, Q., Realizing Interfacial Electron/Hole Redistribution and Superhydrophilic Surface through Building Heterostructural 2 nm CoSe-NiSe Nanograins for Efficient Overall Water Splittings. *Small Methods* **2022**, *6*, 2200459, DOI: 10.1002/smtd.202200459.

[7] Murat, M.; Akkerman, A.; Barak, J., Spatial distribution of electron-hole pairs induced by electrons and protons in SiO. *IEEE Trans. Nucl. Sci*. **2004**, *51*, 3211-8, DOI: 10.1109/TNS.2004.839148.

[8] Hamaguchi, C., Electron and hole mobilities of GaN with bulk, quantum well, and HEMT structures. *J. Appl. Phys*. **2021**, *130*, 125701, DOI: 10.1063/5.0060630.

[9] Ponomarenko, L. A.; Principi, A.; Niblett, A. D., Extreme electron-hole drag and negative mobility in the Dirac plasma of graphene. *Nat. Commun*. **2024**, *15*, 9869, DOI: 10.1038/s41467-024-54198-x.

[10] Allain, A.; Kis, A., Electron and Hole Mobilities in Single-Layer WSe_2. *ACS Nano* **2014**, *8*, 7180-5, DOI: 10.1021/nn5021538.

[11] Gao, J.; Wang, Y.; Liu, Y., Enhancing dielectric permittivity for energy-storage devices through tricritical phenomenon. *Sci. Rep*. **2017**, *7*, 40916, DOI: 10.1038/srep40916.

[12] Ding, S.; Jia, J.; Xu, B., Overrated energy storage performances of dielectrics seriously affected by fringing effect and parasitic capacitance. *Nat. Commun*. **2025**, *16*, 608, DOI: 10.1038/s41467-025-55855-5.

[13] Lee, S. Y.; Kim, H.; Baek, C.; Park, K. I.; Lee, G. J.; Kim, S. H., Yielding optimal dielectric energy storage and breakdown properties of lead-free pyrochlore ceramics by grain refinement strategies. *J. Alloys Compd*. **2024**, *1008*, 176569, DOI: 10.1016/j.jallcom.2024.176569.

[14] Amini, S.; Azami, S. M., Asymmetric deformation density analysis in carbon nanotubes. *Int. J. Quantum Chem*. **2020**, *120*, e26277, DOI: 10.1002/qua.26277.

[15] Salehfar, S.; Azami, S. M., Asymmetric electronic deformation in graphene molecular capacitors. *Int. J. Quantum Chem*. **2024**, *124*, e27426, DOI: 10.1002/qua.27426.

[16] Gasenkova, I. V.; Zhitinskaya, M. K.; Nemov, S. A., Electron density redistribution in Sn-doped Bi_2Te_3. *Phys. Solid State* **1999**, *41*, 1805-8, DOI: 10.1134/1.1131102.

[17] Wang, J.; Kang, J.; Gu, Z. Y.; Liang, Q.; Zhao, X.; Wang, X., Localized Electron Density Redistribution in Fluorophosphate Cathode: Dangling Anion Regulation and Enhanced Na-Ion Diffusivity for Sodium-Ion Batteries. *Adv. Funct. Mater*. **2022**, *32*, 2109694, DOI: 10.1002/adfm.202109694.

[18] Shen, H.; Wang, H.; Wang, T.; Zhang, J.; Yang, S.; Jiang, H., Redistributing the local electron density of bismuth via introducing halogen atoms for boosting CO_2 reduction to formate. *Chem. Catal*. **2024**, *4*, 101057, DOI: 10.1016/j.checat.2024.101057.

[19] Liu, Y. M.; Hou, H.; Zhou, Y. Z., Nanographenes as electron-deficient cores of donor-acceptor systems. *Nat. Commun*. **2018**, *9*, 1901, DOI: 10.1038/s41467-018-04321-6.

[20] Andijani, N.; Al-Qurashi, O.; Wazzan, N.; Irfan, A., Modeling of efficient pyrene-core substituted with electron-donating groups as hole-transporting materials in perovskite solar cells. *Sol. Energy* **2019**, *188*, 898-912, DOI: 10.1016/j.solener.2019.06.074.

[21] Apebende, C. G.; Idante, P. S.; Magu, T. O.; Asogwa, F. C.; Onyebuenyi, I. B.; Unimuke, T. O., Density functional theory study of the influence of activating and deactivating groups on Naphthalene. *Results Chem*. **2022**, *4*, 100669, DOI: 10.1016/j.rechem.2022.100669.

[22] Sutradhar, T.; Misra, A., Role of Electron-Donating and Electron-Withdrawing Groups in Tuning the Optoelectronic Properties of Difluoroboron-Napthyridine Analogues. *J. Phys. Chem. A* **2018**, *122*, 4111-20, DOI: 10.1021/acs.jpca.8b00261.

[23] Barnaveli, A.; Roij, R. V., Asymmetric rectified electric fields: nonlinearities and equivalent circuits. *Soft Matter* **2024**, *20*, 704-16, DOI: 10.1039/D3SM01306E.

[24] Li, L. H.; Tian, T.; Cai, Q., Asymmetric electric field screening in van der Waals heterostructures. *Nat. Commun*. **2018**, *9*, 1271, DOI: 10.1038/s41467-018-03592-3.

[25] Higuchi, K.; Naito, T.; Uedono, A.; Shiraishi, K.; Torii, K.; Boero, M., Asymmetric Distribution of Charge Trap in HfO_2-Based High-k Gate Dielectrics. *ECS Trans*. **2006**, *1*, 777, DOI: 10.1149/1.2209323.

[26] Liu, N.; Jiang, J.; Xu, M.; Zhang, S.; Zhang, R.; Chen, Z., Asymmetric Charge Distribution in One-Dimensional Metal-Organic Assemblies to Promote Photocatalytic Hydrogen Evolution. *ChemSusChem* **2025**, *18*, e202401338, DOI: 10.1002/cssc.202401338.

[27] Huang, L.; Lu, R.; Zhang, W.; Fan, Y.; Du, Y.; Ni, K., Precisely Regulating Asymmetric Charge Distribution by Single-Atom Central Doped Ag-Based Series Clusters for Enhanced Photoreduction of CO_2 to Alcohol Fuels. *Angew. Chem. Int. Ed. Engl*. **2024**, *63*, e202412964, DOI: 10.1002/anie.202412964.

[28] Zimmermann, J. E.; Kim, Y. D.; Hone, J. C.; Höfer, U.; Mette, G., Directional ultrafast charge transfer in a $WSe_2/MoSe_2$ heterostructure selectively probed by time-resolved SHG imaging microscopy. *Nanoscale Horiz*. **2020**, *5*, 1603-9, DOI: 10.1039/D0NH00396D.

[29] Volpert, S.; Hashemi, Z.; Foerster, J. M.; Marques, M. R. G.; Schelter, I.; Kümmel, S., Delocalized electronic excitations and their role in directional charge transfer in the reaction center of Rhodobacter sphaeroides. *J. Chem. Phys*. **2023**, *158*, 195102, DOI: 10.1063/5.0139691.

[30] Lee, C.; Yang, W.; Parr, R. G., Development of the Colle-Salvetti correlation-energy formula into a functional of the electron density. *Phys. Rev. B* **1988**, *37*, 785-9, DOI: 10.1103/PhysRevB.37.785.

[31] Petersson, G. A.; Bennett, A.; Tensfeldt, T. G.; Al-Laham, M. A.; Shirley, W. A.; Mantzaris, J., A complete basis set model chemistry. I. The total energies of closed-shell atoms and hydrides of the first-row atoms. *J. Chem. Phys*. **1988**, *89*, 2193-218, DOI: 10.1063/1.455064.

[32] Mandado, M.; Ramos-Berdullas, N., Analyzing the electric response of molecular conductors using "electron deformation" orbitals and occupied-virtual electron transfer. *J. Comput. Chem*. **2014**, *35*, 1261-9, DOI: 10.1002/jcc.23595.

[33] Ramos-Berdullas, N.; Gil-Guerrero, S.; Mandado, M., Transmission channels in the time-energy uncertainty relation approach to molecular conductance: Symmetry rules for the electron transport in molecules. *Int. J. Quantum Chem*. **2018**, *118*, e25651, DOI: 10.1002/qua.25651.

[34] Gil-Guerrero, S.; Ramos-Berdullas, N.; Pendás, M. Á.; Francisco, E.; Mandado, M., Anti-ohmic single molecule electron transport: is it feasible? *Nanoscale Adv*. **2019**, *1*, 1901-13, DOI: 10.1039/C8NA00384J.

[35] Gil-Guerrero, S.; Ramos-Berdullas, N.; Mandado, M., Can aromaticity enhance the electron transport in molecular wires? *Org. Electron*. **2018**, *61*, 177-84, DOI: 10.1016/j.orgel.2018.05.043.

[36] Gil-Guerrero, S.; Otero, N.; Pena-Gallego, A.; Mandado, M., Unimolecular Electrical Rectification Understood Through Electron Deformation Orbitals. *J. Phys. Chem. C* **2020**, *124*, 17924-31, DOI: 10.1021/acs.jpcc.0c04219.

[37] Gaussian 16, Revision C.01, Frisch, M. J.; Trucks, G. W.; Schlegel, H. B.; Scuseria, G. E.; Robb, M. A.; Cheeseman, J. R.; Scalmani, G.; Barone, V.; Petersson, G. A.; Nakatsuji, H.; Li, X.; Caricato, M.; Marenich, A. V.; Bloino, J.; Janesko, B. G.; Gomperts, R.; Mennucci, B.; Hratchian, H. P.; Ortiz, J. V.; Izmaylov, A. F.; Sonnenberg, J. L.; Williams-Young, D.; Ding, F.; Lipparini, F.; Egidi, F.; Goings, J.; Peng, B.; Petrone, A.;

Henderson, T.; Ranasinghe, D.; Zakrzewski, V. G.; Gao, J.; Rega, N.; Zheng, G.; Liang, W.; Hada, M.; Ehara, M.; Toyota, K.; Fukuda, R.; Hasegawa, J.; Ishida, M.; Nakajima, T.; Honda, Y.; Kitao, O.; Nakai, H.; Vreven, T.; Throssell, K.; Montgomery, J. A., Jr.; Peralta, J. E.; Ogliaro, F.; Bearpark, M. J.; Heyd, J. J.; Brothers, E. N.; Kudin, K. N.; Staroverov, V. N.; Keith, T. A.; Kobayashi, R.; Normand, J.; Raghavachari, K.; Rendell, A. P.; Burant, J. C.; Iyengar, S. S.; Tomasi, J.; Cossi, M.; Millam, J. M.; Klene, M.; Adamo, C.; Cammi, R.; Ochterski, J. W.; Martin, R. L.; Morokuma, K.; Farkas, O.; Foresman, J. B.; Fox, D. J. Gaussian, Inc., Wallingford CT, 2016.

[38] Azami, S. M., Densitizer Ver. 2.0.0. URL: https://orbital.xyz.

[39] GaussView, Ver. 6, Dennington, Roy; Keith, T.; Millam, J., Semichem Inc., Shawnee Mission, KS, **2016**.